Equilibrium Composition of a Plasma in the Low Voltage Air Circuit Breaker Contaminated by the Vapor of AgSnO$_2$ Alloy Electrical Contacts

Banouga Adjigkiga, Kagoné Abdoul Karim, Yaguibou Wêpari Charles, Kohio Niéssan, Koalaga Zacharie, Zougmoré François

Laboratoire de Matériaux et Environnement (LAME), Ecole Doctorale Sciences et Technologies, Université Joseph KI ZERBO, Ouagadougou, Burkina Faso
Email: banougaadjigkiga3@gmail.com

Abstract

When the circuit breaker cuts the electric current, an electric arc is created between its electrodes. The success or failure of breaking the electric current by the circuit breaker depends strongly on the physico-chemical properties of the electric arc created, such as the composition of which depends on the material of the electrical contacts. In this work, we determine the equilibrium composition of the electric arc in the low voltage air circuit breaker with silver tin dioxide alloy contacts, in a temperature range from 500 K to 15,000 K and at atmospheric pressure. We use the **Gibbs** free energy minimization method and develop a computer code to determine the equilibrium composition of the created plasma. The analysis of the results obtained shows that O$_2$ particles with a dissociation energy of 5.114 eV, NO with a dissociation energy of 6.503 eV, and N$_2$ dissociation 9.756 eV dissociate around 3500 K, 5000 K, and 7500 K, respectively. We note that the electro-neutrality is established between the electrons and the cations: Ag$^+$ and NO$^+$, for temperatures lower than 6500 K. For temperatures higher than 6500 K, the electro-neutrality is established between the electrons and the cations: N$^+$, O$^+$, and Ag$^+$. The numerical density of the electrons increases when the proportion of the vapor of the electrical contacts increases in the mixture, in particular for temperatures lower than 11,000 K.

Keywords

Plasma, Electric Arc, **Gibbs** Free Energy, Circuit Breaker, Electrical Contacts, AgSnO$_2$

1. Introduction

Switching devices such as circuit breakers play a very important role in the transport and distribution networks of electrical energy from the various production plants to the users. Indeed, the circuit breaker is the protection element by excellence which has the possibility of de-energizing an electrical circuit by instantly cutting off the current in the event of anomalies. The circuit breaker can prevent fires usually caused by these anomalies.

When the electric current is cut in a circuit breaker, an electric arc is created between its electrodes. This electric arc will generate a plasma which can be defined as a medium made up of a set of particles (atoms, molecules, electrons, radical ions) totally or partially ionized and electrically neutral.

The electric arc and the plasma have been the subject of numerous theoretical and experimental studies [1] [2] [3] [4] [5]. Studies have shown that the nature of the electrodes (electrical contacts) significantly modifies the behavior of the electric arc [6].

Circuit breaker contact materials have various qualities. There is no ideal material. Thus, the choice of the material constituting the electrodes is crucial and must above all be adapted to the intended application.

In this work, we are interested in the equilibrium composition of the plasma in the low voltage air circuit breaker with silver tin dioxide alloy contacts. The reason is that this type of contact has a high resistance to electric arc erosion and has good anti-weld properties [6].

We use the **Gibbs** free energy minimization method and we develop a computer code to determine the equilibrium composition of the created plasma.

After the introduction in Section 1, we give the materials and methods in Section 2. The results, analyses, and discussions are given in Section 3. Finally, we present the conclusion in Section 4.

2. Materials and Methods

2.1. Choice of Electrical Contact Material

The materials used for contacts in breaking devices are mainly copper and silver due to their low contact resistance. If the latter is used in their pure state, they undergo substantial erosion and tend to weld together under the effect of strong electric currents. To avoid this, manufacturers manufacture electrical contacts from metal alloys or pseudo-alloys in the form of solid rivets. They are mainly composed of AgC, AgNi, AgW, AgWC, CuCr, and $AgSnO_2$.

The materials used in the development of electrical contacts must have well-defined properties, in order to have a long life and to be resistant to various stresses with significant temperature which rises until melting and the formation of droplets. Therefore, they must satisfy the following properties [7]:
- Have adequate melting temperatures;
- Have high electrical and thermal conductivities;
- Be sufficiently inert with respect to the atmosphere in which they will be

placed to avoid the formation of insulating films;

- Have sufficient mechanical properties to withstand the forces applied when the contacts are crushed.

In addition, the electrical contacts depend on several parameters such as the nature of the circuit (resistive, inductive), the type of electric arc (opening or closing), the type of current (direct or alternating current), and the intensity (low or strong). This is why the choice of alloy for electrical contact materials is tricky.

Silver is preferentially used for high-intensity electrical contact pads, despite its higher cost, because it has a lower electrical resistivity (1.59 $\mu\Omega\cdot$cm) and high thermal conductivity (419 W·m^{-1}·K^{-1}) at room temperature (20˚C) [6]. In addition, silver is a noble metal that does not oxidize in the air, unlike copper and aluminum.

However, its use remains limited due to its tendency to weld and its low resistance to erosion. Indeed, its poor resistance to erosion is linked to its low melting temperature (961˚C) and its low boiling temperature (2212˚C). This is why silver is associated with other metals (Cu, Ni, C, W) or oxides (CdO, SnO$_2$, ZnO) to form pseudo-alloys in order to improve the resistance to welding and to erosion, when the electric current is cut off, without altering the resistance of the electric contact [6] [8] [9]. Metal oxides of the SnO$_2$ type (3.3% to 5% maximum 14%) are intended to reduce the risks of welding in the breaking device, but their addition in large quantities greatly increases the duration of the electric arc, thus aggravating the contact erosion [6].

We choose to use the alloy of silver and tin dioxide (AgSnO$_2$) because it has a high resistance to electric arc erosion and has good anti-welding properties [6] [8] [9].

2.2. Method for Determining the Equilibrium Composition of Plasma

In this work, we use the **Gibbs** free energy minimization method. This method is very effective and easy to implement. It is also adapted to the type of plasma studied.

However, it requires knowledge of the specific thermodynamic data of all the chemical species that make up the mixture. It was developed by **White**, **Johnson** and **Dantzig** at full thermodynamic equilibrium [10]. **Lagrange** multipliers are used to minimize the Gibbs free energy (free enthalpy), resulting in the convergence of results.

The determination of the equilibrium composition requires prior knowledge of the specific chemical potentials of all the particles populating the plasma. We used data from **NIST**, **Bonnie**, **F. Bendjebbar** and **JANAF** tables to determine the specific chemical potentials of electrons, atomic and molecular species [2] [11] [12]. We also use the thermodynamic data smoothed and tabulated by Bonnie for the calculation of the specific thermodynamic properties. This data is for standard enthalpy and standard entropy. Enthalpy and entropy are derived from

the standard heat capacity.

The thermodynamic data are dependent on the temperature and are determined at the pressure of 1 bar.

The heat capacity is given by the relation [12] [13]:

$$\frac{C_{P,i}^0(T)}{R} = a_{1,i}T^{-2} + a_{2,i}T^{-1} + a_{3,i} + a_{4,i}T + a_{5,i}T^2 + a_{6,i}T^3 + a_{7,i}T^4 \tag{1}$$

Enthalpy and entropy are obtained by integrating with respect to temperature respectively $C_{P,i}^0(T)$ and $C_{P,i}^0(T)/T$:

$$\frac{H_i^0(T)}{RT} = -a_{1,i}T^{-2} + a_{2,i}\frac{\ln(T)}{T} + a_{3,i} + a_{4,i}\frac{T}{2} \\ + a_{5,i}\frac{T^2}{3} + a_{6,i}\frac{T^3}{4} + a_{7,i}\frac{T^4}{5} + \frac{b_{1,i}}{T} \tag{2}$$

$$\frac{S_i^0(T)}{R} = -a_{1,i}\frac{T^{-2}}{2} - a_{2,i}T^{-1} + a_{3,i}\ln(T) + a_{4,i}T \\ + a_{5,i}\frac{T^2}{2} + a_{6,i}\frac{T^3}{3} + a_{7,i}\frac{T^4}{4} + b_{2,i} \tag{3}$$

The specific chemical potential is given by the relation:

$$\mu_i^0 = H_i^0 - T*S \tag{4}$$

where $a_{j,i}(j=1,\cdots,7)$ represent the smoothing constants of $C_{p,i}^0$, S_i^0 and h_i^0. $b_{j,i}$ the integration constants of the particle i, R the ideal gas constant and T the temperature in kelvin. The constants $a_{j,i}$ and $b_{j,i}$ of certain particles are taken from the work of **Bonnie** [12].

We use the following hypotheses:
- The composition of the air, in mass percentage, is taken as 77.8% nitrogen and 22.2% oxygen;
- The other constituents of the air are negligible;
- The range of temperatures considered is from 500 K to 15,000 K and at atmospheric pressure;
- The different percentages retained are mass percentages;
- The different species of the plasma are characterized by a single temperature.

In the case of the calculation of the equilibrium composition of plasmas of mixtures of air, silver and tin dioxide, we have retained five types of basic nuclei (four basic elements and electrons): Ag, N, O, Sn and e⁻.

Practical studies have shown that silver oxide (Ag_2O) dissociates from 430 K. The latter is eliminated when the electric arc appears.

The chemical particles taken into account in the plasma of mixtures of air, silver and tin dioxide are:
- The electron and the monatomic particles are in total seventeen (17):
  e⁻, Ag⁻, N⁻, O⁻, Sn⁻, Ag, N, O, Sn, Ag⁺, N⁺, O⁺, Sn⁺, Ag²⁺, N²⁺, O²⁺, Sn²⁺;
- The diatomic particles are a total of eleven (11):
  N_2^-, O_2^-, NO⁻, NO, N_2, O_2, SnO, Sn_2, NO⁺, N_2^+, O_2^+;
- The triatomic particles and more are a total of twelve (12):

NO_3^-, NO_2^-, N_2O_5, N_2O_4, N_2O_3, NO_3, NO_2, N_2O, N_3, O_3, SnO_2, N_2O^+.

We have a total of forty (40) chemical particles.

First, we determine the numbers of moles, and then this will allow us to calculate the densities of the different particles. At a given point, the numerical densities of the chemical species, symbolized by $Y(y_1, y_2, y_3, \cdots, y_M)$, must satisfy electrical neutrality and conservation of the number of nuclei in the plasma. These conditions result in the following relation [14] [15] [16] [17]:

$$\sum_{i=1}^{M} a_{ij} y_j = b_j \ (j = 1, 2, \cdots, m) \tag{5}$$

where M is the number of chemical species in the mixture, m the number of basic nuclei including the electron and a_{ij} represents the matrix containing the number of nuclei and electrical charges of the chemical species taken into account in this work, in other words, a_{ij} corresponds to the number of type nuclei j of the particle i and b_j the initial number of type nuclei j.

The calculated **Gibbs** free energy at the point $Y(y_1, y_2, y_3, \cdots, y_M)$ is given by [18] [19]:

$$G(Y) = \sum_{i=1}^{M} y_i \left(\mu_i^0 + RT \ln\left(\frac{P}{P^0}\right) + RT \ln\left(\frac{y_i T}{\sum_{k=1}^{M} y_k T}\right) \right) \tag{6}$$

The values y_i are proportional to the numerical densities n_i.

We need to find the point $Y(y_1, y_2, y_3, \cdots, y_M)$ that minimizes the function $G(Y)$ and for which the coordinates y_i satisfy the following conditions:

- The numbers of moles must be positive $y_i \geq 0$, $\forall i$;
- The coordinates y_i must satisfy the conservation of the number of nuclei and electrical neutrality.

To obtain the direction in which G decreases, **White** *et al.* perform a Taylor series expansion of order two (02) at the point, which gives:

$$Q(X) = G(Y) + \sum_{i}^{M} \left(\frac{\partial G}{\partial x_i}\right)_{X=Y} (x_i - y_i) + \frac{1}{2} \sum_{i=1}^{M} \sum_{k=1}^{M} \left(\frac{\partial^2 G}{\partial x_i \partial y_k}\right)_{X=Y} (x_i - y_i)(x_k - y_k) \tag{7}$$

Taking into account the physical conditions of Equation (5), we introduce the **Lagrange** multipliers π_j. So we get the function $\zeta(X)$:

$$\zeta(X) = Q(X) + \sum_{j=1}^{m} \pi_j \left(-\sum_{i=1}^{M} a_{ij} y_i + b_j \right) \tag{8}$$

$G(X)$ is then minimal when we have [10] [20]:

$$\frac{\partial \zeta(X)}{\partial x_i} = RT \left(C_i + RT \ln\left(\frac{y_i T}{\sum_{k=1}^{M} y_k T}\right) \right) + RT \left[\frac{x_i}{y_i} - \frac{\sum_{k=1}^{M}(x_k - y_k)T}{\sum_{k=1}^{M} y_k T} \right] - \sum_{i=1}^{m} \pi_j a_{ij} = 0 \tag{9}$$

with:

$$C_i = \mu_i^0 + RT \ln\left(\frac{P}{P^0}\right) \tag{10}$$

Using the **Newton**-**Raphson** method, we obtain the following system of equations [2] [13] [18] [21] [22]:

$$
\begin{pmatrix}
\dfrac{RT}{y_1} & \cdots & 0 & a_{11} & \cdots & a_{1m} \\
\vdots & \ddots & \vdots & \vdots & \ddots & \vdots \\
0 & \cdots & \dfrac{RT}{y_M} & a_{M1} & \cdots & a_{Mm} \\
a_{11} & \cdots & a_{M1} & 0 & \cdots & 0 \\
\vdots & \ddots & \vdots & \vdots & \ddots & \vdots \\
a_{1m} & \cdots & a_{Mm} & 0 & \cdots & 0
\end{pmatrix}
\begin{pmatrix}
\Delta_{x_1} \\ \vdots \\ \Delta_{x_M} \\ \Delta\pi_1 \\ \vdots \\ \Delta_m
\end{pmatrix}
=
\begin{pmatrix}
-\mu_1^0 - RT\ln\left(\dfrac{y_1 T}{\sum_{k=1}^M y_k T}\right) - RT\ln\left(\dfrac{P}{P_0}\right) - \sum_{j=1}^m \pi_i a_{ij} \\
\vdots \\
-\mu_M^0 - RT\ln\left(\dfrac{y_M T}{\sum_{k=1}^M y_k T}\right) - RT\ln\left(\dfrac{P}{P_0}\right) - \sum_{j=1}^m \pi_i a_{ij} \\
-\sum_{i=1}^M a_{i1} y_i + b_1 \\
\vdots \\
-\sum_{i=1}^M a_{im} y_i + b_m
\end{pmatrix}
\quad (11)
$$

The electric neutrality, in the plasmas of electric arcs, being established we can suppose that $b_1 = 0$ (b_1 is the number of initial electron).

We take into account forty chemical species and five different types of nuclei which correspond to the five (05) **Lagrange** multipliers, that is to say that $M = 40$ and $m = 5$. The system of Equations (11) is therefore a system of forty-five (45) equations with forty-five unknowns, which are the numbers of moles of the forty chemical species plus the five **Lagrange** multipliers.

The principle of the numerical method consists to assign initially and arbitrarily the moles numbers values y_i and to the five Lagrange multipliers. The numbers of moles must satisfy the following two conditions:

$$
\begin{cases}
y_i \geq 0 & \forall i \\
\sum_{i=1}^M a_{ij} y_i = b_j & j = 1, \cdots, m
\end{cases}
\quad (12)
$$

For the resolution of the system of Equations (11), the new values of the numbers of moles and the **Lagrange** multipliers are obtained by the following relation:

$$
\begin{cases}
x_i = y_i + \lambda \Delta y_i & \forall i \in [1; M] \\
\pi_j = \pi_j + \lambda \Delta \pi_j & \forall j \in [1; m]
\end{cases}
\quad \lambda \in [0;1]
\quad (13)
$$

The parameter λ is the correction coefficient. It allows avoiding the negative values of the numbers of moles which can appear when one moves away from the solution. To avoid exceeding the convergence point, λ must satisfy the following condition:

$$
\frac{dG(\lambda)}{d\lambda} \prec 0
\quad (14)
$$

with:

$$
\frac{dQ(\lambda)}{d\lambda} = \sum_{i=1}^M (x_i - y_i)\left(C_i + RT\ln\left(\frac{y_i + \lambda(x_i - y_i)T}{\sum_{k=1}^M (y_k + \lambda(x_k + y_k)T)}\right)\right)
\quad (15)
$$

Equation (14) translates that:

$$
x_i = y_i + \lambda \Delta y_i \succ 0 \quad \forall i \in [1; M]
\quad (16)
$$

The new values of number of moles and **Lagrange** multipliers are used for a new cycle of calculation. The criterion for interrupting iterations is set by the following condition given by **Cayet** [13] [20]:

$$\frac{G(X)-G(Y)}{G(X)} \prec 10^{-14} \tag{17}$$

Starting point values y_i do not obey Dalton's law. The values obtained after convergence are proportional to the volume densities n_i.

The proportionality constant is calculated with **Dalton**'s law by [13]:

$$n_i = x_i \frac{\dfrac{P-\Delta P}{k}}{\displaystyle\sum_{i=1}^{M} y_i T} \tag{18}$$

where P is the total pressure of the mixture and ΔP the pressure drop resulting from the **Coulomb** attraction produced between the charged particles.

3. Results, Analyzes, and Discussions

3.1. Results

In this part, first, we present the calculation results of the equilibrium composition of the pure air plasma.

Next, we present the results of calculating the equilibrium composition of plasmas of mixtures of air, silver and tin dioxide assuming that the electrical contact material (the $AgSnO_2$ alloy) contains four percent of tin dioxide (4% SnO_2).

Finally, we show the influence of vapor from electrical contacts on the numerical densities of electrons and the four basic elements.

Figures 1-3 present the evolutions of the numerical densities according to the temperature, of the particles populating these plasmas, at atmospheric pressure and at local thermodynamic equilibrium (LTE).

Figure 4 shows the influence of vapor from electrical contacts in $AgSnO_2$ on the numerical densities of electrons and the four basic elements.
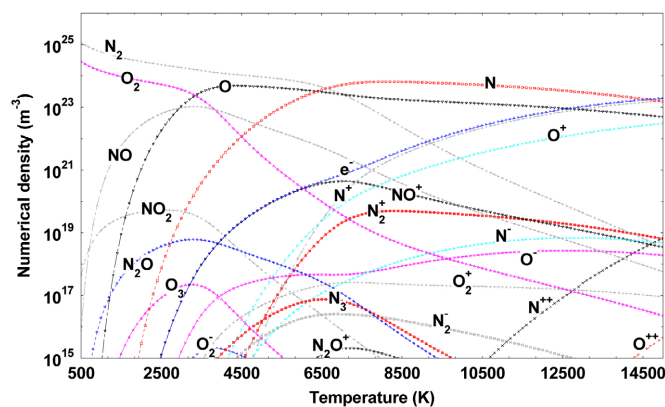

Figure 1. Evolution as a function of temperature of the numerical densities of particles in pure air plasma at atmospheric pressure and at LTE.

Figure 2. Evolution as a function of temperature of the numerical densities of plasma particles at 99.99% air and 0.01% AgSnO$_2$, with 4% SnO$_2$ in the alloy, at atmospheric pressure and at LTE.

Figure 3. Evolution as a function of temperature of the numerical densities of plasma particles at 95% air and 5% AgSnO$_2$, with 4% SnO$_2$ in the alloy, at atmospheric pressure and at LTE.

Figure 4. Influence of vapor from electrical contacts on the numerical densities of electrons and the four basic elements.

3.2. Analyses and Discussions

To validate the computer code that we have developed, we compare our values of numerical densities of some particles, from the air plasma at atmospheric pressure and the ETL (Figure 1), with those published by **KOHIO** *et al.* [18] for two temperature values (8000 K and 10,000 K). The results presented in Table 1 show that our results are in good agreement with those of **KOHIO** *et al.* [18].

The differences observed, in the order of 0% to 14% maximum, may be due, on the one hand, to the fact that we did not use exactly the same data for the calculation.

On the other hand, by the fact that **KOHIO** *et al.* used the volume percentage while we used the mass percentage since, in this work, we are more interested in the masses of the different particles than in their volumes.

The analysis of these different figures shows that the numerical densities of the particles: Ag, N, O and Sn, as well as the particles which are formed from a combination of these basic elements, depend closely on the initial proportions of the mixture.

By examining the different results of Figure 2 and Figure 3, we observe that:

- For temperatures below 1500 K, the main particles are: N_2, O_2, Ag and SnO;
- For temperatures between 1500 K and 6500 K, the main particles are: NO, O, Sn and NO^+;
- For temperatures above 6500 K, the main particles are: e^-, N, N^+, O^+, Ag^+ and Sn^+.

We note that the electro-neutrality is established between the electrons and the cations: Ag^+ and NO^+, for temperatures lower than 6500 K. For temperatures above 6500 K, electro-neutrality is established between the electrons and the cations: N^+, O^+ and Ag^+.

Table 1. Comparison of our composition calculation results, of air plasma at ETL and at atmospheric pressure, with those of **KOHIO** *et al.* [18].

Particules	8000 K			10,000 K		
	KOHIO	this study	difference%	KOHIO	this study	difference%
e^-	2.18E+21	2.19E+21	0.45%	1.67E+22	1.71E+22	2.39%
O_2	8.41E+18	7.77E+18	7.60%	1.24E+18	1.08E+18	12.90%
NO	6.63E+20	7.05E+20	6.33%	6.26E+19	6.75E+19	7.82%
N	5.89E+23	6.54E+23	11.01%	4.97E+23	5.49E+23	10.46%
N_2	4.91E+22	5.53E+22	12.62%	1.93E+21	2.17E+21	12.43%
O^+	4.07E+20	3.53E+20	13.26%	2.78E+21	2.41E+21	13.30%
N^+	1.34E+21	1.51E+21	12.68%	1.31E+22	1.46E+22	8.95%
O	2.02E+23	1.90E+23	5.94%	1.47E+23	1.39E+23	5.44%

Electronegative particles (anions): N_2^-, O^-, N^- and O_2^- appear with low densities. Nevertheless, these anions could have a significant influence on the electrical conductivity, because these particles capture the electrons and reduce not only the number of electrons but also their mobility.

We notice that the O_2 particle, with a dissociation energy of 5.114 eV, dissociates around 3500 K. The NO particle, with a dissociation energy of 6.503 eV, dissociates around 5000 K. The N_2 particle which has a dissociation energy of 9.756 eV higher than the last two particles dissociates around 7500 K. Thus, we can say that the dissociation temperature of a particle depends on its dissociation energy.

Moreover, in these plasmas, we observe that, for the same temperature, the numerical densities of the Sn^{2+} particles are greater than the numerical densities of the Ag^{2+} particles. This can be explained by the fact that the second ionization energy of tin (14.63 eV) is lower than that of silver (21.49 eV). Similarly, the numerical densities of N^{2+} particles are higher than the numerical densities of O^{2+} particles. This can be explained by two factors. The first factor is that the second ionization energy of nitrogen (29.60 eV) is lower than that of oxygen (35.11 eV). The second one is due to the fact that the percentage of nitrogen is greater than that of oxygen in the initial proportion.

According to these different figures, we notice that the poly-atomic particles such as NO_3, N_2O_4, N_2O_3, N_2O_5, NO_3^- do not appear, that is to say, that their numerical densities are lower than the numerical minimum density that we considered (10^{15} m^{-3}). Indeed these particles dissociate when the temperature increases because their dissociation energies are very low. It is the same for the particles: O_3, N_3 which only appear at very low temperatures with low numerical densities ($n_i \prec 10^{19}$ m^{-3}).

The analysis of Figure 4 shows that for the same temperature, the numerical densities of silver atoms and tin increase when the percentage of the particles coming from the vapor of the electric contacts increases, while the atoms of nitrogen and oxygen decrease slightly. Indeed the numerical densities of particles such as Ag and Sn, for the same temperature, increase when the proportion, in mass percentage, of the vapor of the electrical contacts ($AgSnO_2$) increases in the mixture. It is the same for the particles: Ag^+, Sn^+, Ag^{2+} and Sn^{2+}.

However, the numerical densities of particles such as N, O, N_2, O_2, N^+, O^+, N^{2+}, and O^{2+} for the same temperature, decrease slightly when the proportion, in mass percentage, of the vapor from the electrical contacts increases.

As for the numerical density of the electrons, it increases when the proportion, in mass percentage, of the vapor of the electrical contacts increases in the mixture, for temperatures lower than 11,000 K, which could lead to an increase in the electrical conductivity of the electric arc.

4. Conclusions

The composition of the plasma in the low voltage air circuit breaker with silver

tin dioxide alloy contact is determined in a temperature range from 500 K to 15,000 K and at atmospheric pressure.

We used the **Gibbs** free energy minimization method. It allowed us to develop a computer code, from which we determined the equilibrium composition of the plasma created.

The results obtained show that electro-neutrality is established between electrons and cations: Ag^+, and NO^+, for temperatures below 6500 K. For temperatures above 6500 K, electro-neutrality is established between electrons and cations: N^+, O^+ and Ag^+. The density of the electrons increases when the proportion, in mass percentage, of the vapor of the electrical contacts increases in the mixture, in particular for temperatures lower than 11,000 K. As the density of the electrons increases, this could lead to an increase in the electrical conductivity of the electric arc. The determination of the thermodynamic properties and transport coefficients are therefore necessary to verify this hypothesis.

Conflicts of Interest

The authors declare no conflicts of interest regarding the publication of this paper.

References

[1] Abbaoui, M., Cheminat, B. and Andanson, P. (1985) Influence de la nature du metal sur la conductivité d'un plasma argon-métal. *Journal of Physics D: Applied Physics*, **18**, L159-L165. https://doi.org/10.1088/0022-3727/18/10/002

[2] Bendjebbar, F., André, P., Benbakkar, M., Rochette, D., Flazi, S. and Vacher, D. (2012) Plasma Formed in Argon, Acid Nitric and Water Used in Industrial ICP Torches. *Plasma Science and Technology*, **14**, 683. https://doi.org/10.1088/1009-0630/14/8/01

[3] Cheminat, B. and Andanson, P. (1985) La conduction dans la colonne d'un arc électrique contaminée par des vapeurs de cuivre. *Journal of Physics D: Applied Physics*, **18**, L2183-L2192. https://doi.org/10.1088/0022-3727/18/11/008

[4] Abbaoui, M. and Cheminat, B. (1991) Determination of the Characteristics of an Electric Arc Plasma Contaminated by Vapors from Insolators. *IEEE Transactions on Plasma Sciences*, **19**, 1-8. https://doi.org/10.1109/27.62359

[5] Koalaga, Z., Abbaoui, M. and Lefort, A. (1993) Calcul des propriétés thermodynamiques des plasmas d'isolants $C_xH_yO_zN_t$. *Journal of Physics D: Applied Physics*, **26**, 393-403. https://doi.org/10.1088/0022-3727/26/3/008

[6] Choi, E.Y.K. (2015) Etude des arcs and leurs conséquences sur les métaux de contacts électriques de puissance pour des applications D C. Thèse de doctorat, Université de Rennes 1, Rennes.

[7] Khaled, B. (2007) Utilisation des alliages monotectiques dans l'élaboration des contacts électriques. Thèse de doctorat, Université de Batna, Batna.

[8] Jeannot, D., Pinard, J., Ramoni, P. and Jost, E.M. (1994) Physical and Chemical Properties of Metal Oxide Additions to $AgSnO_2$ Contact Materials and Predictions of Electrical Performance. *IEEE Transactions on Components and Packaging Technologies Part A*, **17**, 17-23. https://doi.org/10.1109/95.296363

[9] Abbaoui, M., André, P. and Augeard, A. (2018) Modèle enthalpique de Stephan

pour l'étude du pied d'arc cathodique. *Journal International de Technologie, de l'innovation de la physique, de l'énergieet de l'environnement*, **4**, 1-16. http://dx.doi.org/10.18145/jitipee.v4i1.138

[10] White, W.B., Johnson, S.M. and Dantzig, G.B. (1957) Chemical Equilibrium in Complex Mixtures. *Journal of Chemical Physics*, **28**, 751-755. http://dx.doi.org/10.1063/1.1744264

[11] Chase, M.W. (1998) Nist-Janaf Thermochemical Tables. Fourth Edition, Part I, Al-Co. *Journal Physical Chemical Reference Data*, Monograph No. 9.

[12] McBride, B.J., Zeche, M.J. and Gordon, S. (2002) NASA Glenn Coefficients for Calculating Thermodynamic Properties of Individual Species. Glenn Research Center, Cleveland.

[13] Yaguibou, W.C., Kohio, N., Kagoné, A.K., Koalaga, Z. and Zougmoré, F. (2018) Influence des aérosols sur la composition à l'équilibre d'un plasma d'air. *Journal International de Technologie, de l'innovation de la physique, de l'énergieet de l'environnement*, **4**, 5-19. http://dx.doi.org/10.18145/jitipee.v4i1.167

[14] André, P. (1996) Composition and Thermodynamic Properties of Ablated Vapours of PMMA, PA6-6, PETP, POM and PE. *Journal of Physics D: Applied Physics*, **29**, 1963-1972. https://doi.org/10.1088/0022-3727/29/7/033

[15] André, P., Ondet, J., Pellet, R. and Lefort, A. (1997) The Calculation of Monatomic Spectral Lines' Intensities and Composition in Plasma Out of Thermal Equilibrium; Evaluation of Thermal Disequilibrium in ICP Torches. *Journal of Physics D: Applied Physics*, **30**, 2043-2055. https://doi.org/10.1088/0022-3727/30/14/012

[16] André, P. and Koalaga, Z. (2010) Composition of a Thermal Plasma Formed from PTFE with Copper in Non-Oxidant Atmosphere. Part I: Definition of a Test with the SF_6. *High Temperature Material Processes*, **14**, 279. https://doi.org/10.1615/HighTempMatProc.v14.i3.70 https://hal.archives-ouvertes.fr/hal-00537752

[17] André, P., Courty, M.A., Kagoné, A.K., Koalaga, Z., Kohio, N. and Zougmoré, F. (2016) Calcul de la composition chimique dans un plasma issu de mélanges de PTFE, d'air, de cuivre and de vapeur d'eau dans le cadre d'appareillages de coupure électrique à air. *Journal International de Technologie, de l'innovation de la physique, de l'énergieet de l'environnement*, **2**, 3-8. http://dx.doi.org/10.18145/jitipee.v2i1.128.g70

[18] Kohio, N., Kagoné, A.K., Koalaga, Z. and Zougmoré, F. (2014) Composition of Air-Water Vapor Mixtures at Low Temperatures. *International Journal of Advanced Research in Science, Engineering and Technology*, **1**, 240-246.

[19] André, P. and Lalléchère, S. (2021) Calcul de la permittivité dans un plasma d'air hors de l'équilibre chimique and thermique: Effet sur la propagation des ondes électromagnétiques à différentes altitudes. *Journal International de Technologie, de l'innovation de la physique, de l'énergieet de l'environnement*, **1**, 1-27. https://doi.org/10.52497/jitipee.v7i1.286

[20] Cayet, S. and Dudeck, M. (1996) Equilibre chimique dans des mélanges gazeux en déséquilibre thermique. *Journal de Physique III, EDP Sciences*, **6**, 403-420. https://doi.org/10.1051/jp3:1996130

[21] Rochette, D., Buissière, W. and André, P. (2004) Composition, Enthalpy and Vaporisation Temperature Calculation of $Ag\text{-}SiO_2$ Plasmas with Air in the Temperature Range from 1000 to 6000 K and for Pressure Included between 1 and 50 Bar. *Plasma Chemistry and Plasma Processing*, **24**, 475-492. https://doi.org/10.1007/s11090-004-2280-2

[22] Kohio, N., Kagoné, A.K., Yaguibou, W.C, Koalaga, Z. and Zougmoré, F. (2020) Influence of Metallic Copper Vapors on the Chemical Composition of a Mixture of Air and Water Vapor Thermal Plasmas in the Temperature Range 1000 K to 20000 K. *American Journal of Nano Research and Applications*, **8**, 50-57.
http://www.sciencepublishinggroup.com/j/nano